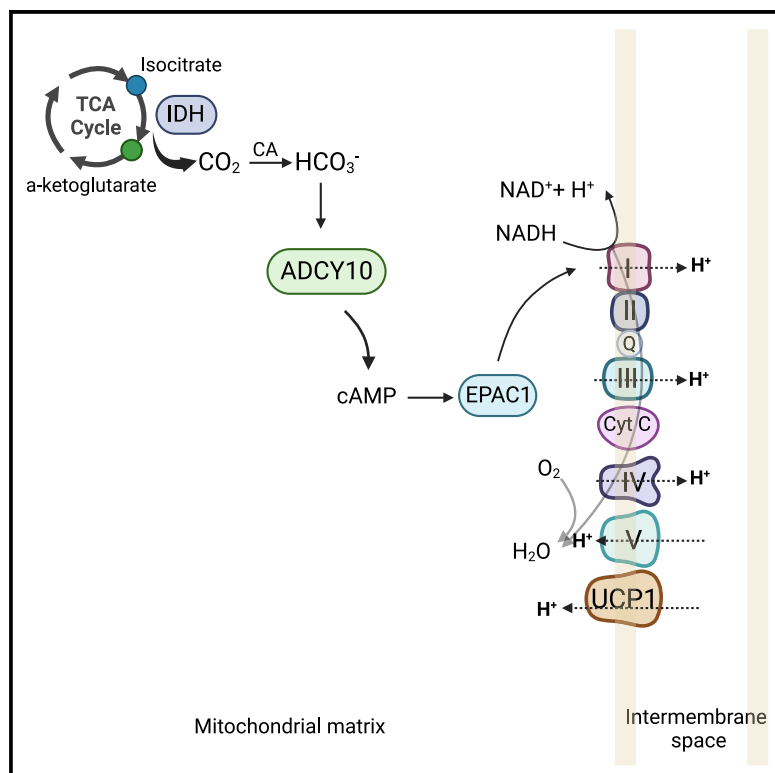


Adenylate cyclase 10 promotes brown adipose tissue thermogenesis

Graphical abstract



Authors

Anupam Das, Christine Mund, Eman Hagag, ..., Triantafyllos Chavakis, Thomas Noll, Vasileia Ismini Alexaki

Correspondence

vasileiaismini.alexaki@uniklinikum-dresden.de

In brief

Physiology; Molecular biology; Cell biology

Highlights

- Cold exposure upregulates IDH activity and ADCY10 expression in brown adipocytes
- IDH inhibition or ADCY10 deficiency reduces cold resistance
- The IDH-ADCY10-cAMP-EPAC1-complex I pathway sustains the $\Delta\Psi_m$ in brown adipocytes



Article

Adenylate cyclase 10 promotes brown adipose tissue thermogenesis

Anupam Das,¹ Christine Mund,² Eman Hagag,² Ruben Garcia-Martin,² Eleftheria Karadima,² Anke Witt,¹ Mirko Peitzsch,² Andreas Deussen,¹ Triantafyllos Chavakis,^{2,3,4} Thomas Noll,¹ and Vasileia Ismini Alexaki^{2,5,*}

¹Department of Physiology, Faculty of Medicine, Technische Universität Dresden, Dresden, Germany

²Institute for Clinical Chemistry and Laboratory Medicine, Faculty of Medicine and University Hospital Carl Gustav Carus, Technische Universität Dresden, Dresden, Germany

³Paul Langerhans Institute Dresden of the Helmholtz Center Munich, University Hospital and Faculty of Medicine, Technische Universität Dresden, Dresden, Germany

⁴German Center for Diabetes Research (DZD), Neuherberg, Germany

⁵Lead contact

*Correspondence: vasileiaismini.alexaki@uniklinikum-dresden.de

<https://doi.org/10.1016/j.isci.2025.111833>

SUMMARY

Brown adipose tissue (BAT) thermogenesis dissipates energy through heat production and thereby it opposes metabolic disease. It is mediated by mitochondrial membrane uncoupling, yet the mechanisms sustaining the mitochondrial membrane potential ($\Delta\Psi_m$) in brown adipocytes are poorly understood. Here we show that isocitrate dehydrogenase (IDH) activity and the expression of the soluble adenylate cyclase 10 (ADCY10), a CO₂/bicarbonate sensor residing in mitochondria, are upregulated in BAT of cold-exposed mice. IDH inhibition or ADCY10 deficiency reduces cold resistance of mice. Mechanistically, IDH increases the $\Delta\Psi_m$ in brown adipocytes via ADCY10. ADCY10 sustains complex I activity and the $\Delta\Psi_m$ via exchange protein activated by cAMP1 (EPAC1). However, neither IDH nor ADCY10 inhibition affect uncoupling protein 1 (UCP1) expression. Hence, we suggest that ADCY10, acting as a CO₂/bicarbonate sensor, mediates the effect of IDH on complex I activity through cAMP-EPAC1 signaling, thereby maintaining the $\Delta\Psi_m$ and enabling thermogenesis in brown adipocytes.

INTRODUCTION

Brown adipose tissue (BAT) has the distinct capacity to generate heat, which is important for maintaining body temperature upon exposure to cold. Brown adipocytes are rich in mitochondria containing high amounts of uncoupling protein 1 (UCP1). UCP1 resides in the inner mitochondrial membrane (IMM) and mediates proton leak through the IMM leading to generation of heat at the expense of ATP production.¹ Its expression is upregulated by β_3 adrenergic signaling upon exposure to cold or intake of energy-rich food.^{1,2} β_3 adrenergic signaling activates transmembrane adenylate cyclases (tmAC), which produce cAMP. This leads to protein kinase A (PKA) activation, which triggers hormone-sensitive triglyceride lipase (HSL)-dependent lipolysis and generation of free fatty acids (FFA), the latter activating UCP1-dependent proton leak.^{3,4} Due to the role of BAT in dissipating energy, recruitment of BAT is viewed as a promising tool to combat obesity and associated metabolic perturbations.^{5–7} Indeed, evidence in humans suggests that BAT thermogenesis associates with improved glucose homeostasis.^{8–10}

Efficient thermogenesis requires elevated mitochondrial respiration in brown adipocytes, which is fueled by the tricarboxylic acid (TCA) cycle intermediate succinate through the function of complex II (succinate dehydrogenase, SDH).¹ In BAT of cold-

exposed animals, succinate is sequestered from the circulation and drives SDH-mediated reactive oxygen species (ROS) production, which promotes thermogenesis.^{1,11} However, the role of the endogenous TCA cycle of brown adipocytes in the regulation of thermogenesis is poorly understood.

Here we show that isocitrate dehydrogenase (IDH) activity increases in BAT upon cold exposure and IDH inhibition impairs cold resistance in mice and mitochondrial function in brown adipocytes. We suggest that CO₂ generated by IDH can activate the soluble adenylate cyclase ADCY10, which localizes in different cellular compartments including mitochondria.^{12,13} In contrast to tmAC, ADCY10 is not regulated by G proteins.^{14–16} Instead, ADCY10 activity is sensitive to local concentrations of ATP, free Ca²⁺ and CO₂/bicarbonate.^{14–16} Previous reports showed that mitochondrial ADCY10 promotes electron transport chain (ETC) function and concomitant ATP production upon sensing bicarbonate.^{17–19} We show that ADCY10 is highly expressed in BAT and its expression is upregulated by cold exposure. ADCY10 deficient mice have impaired cold resistance and ADCY10 inhibition diminishes the mitochondrial membrane potential ($\Delta\Psi_m$) in brown adipocytes. We suggest that the IDH-ADCY10-cAMP axis maintains the $\Delta\Psi_m$ in brown adipocytes thereby supporting UCP1 function and promoting thermogenesis.



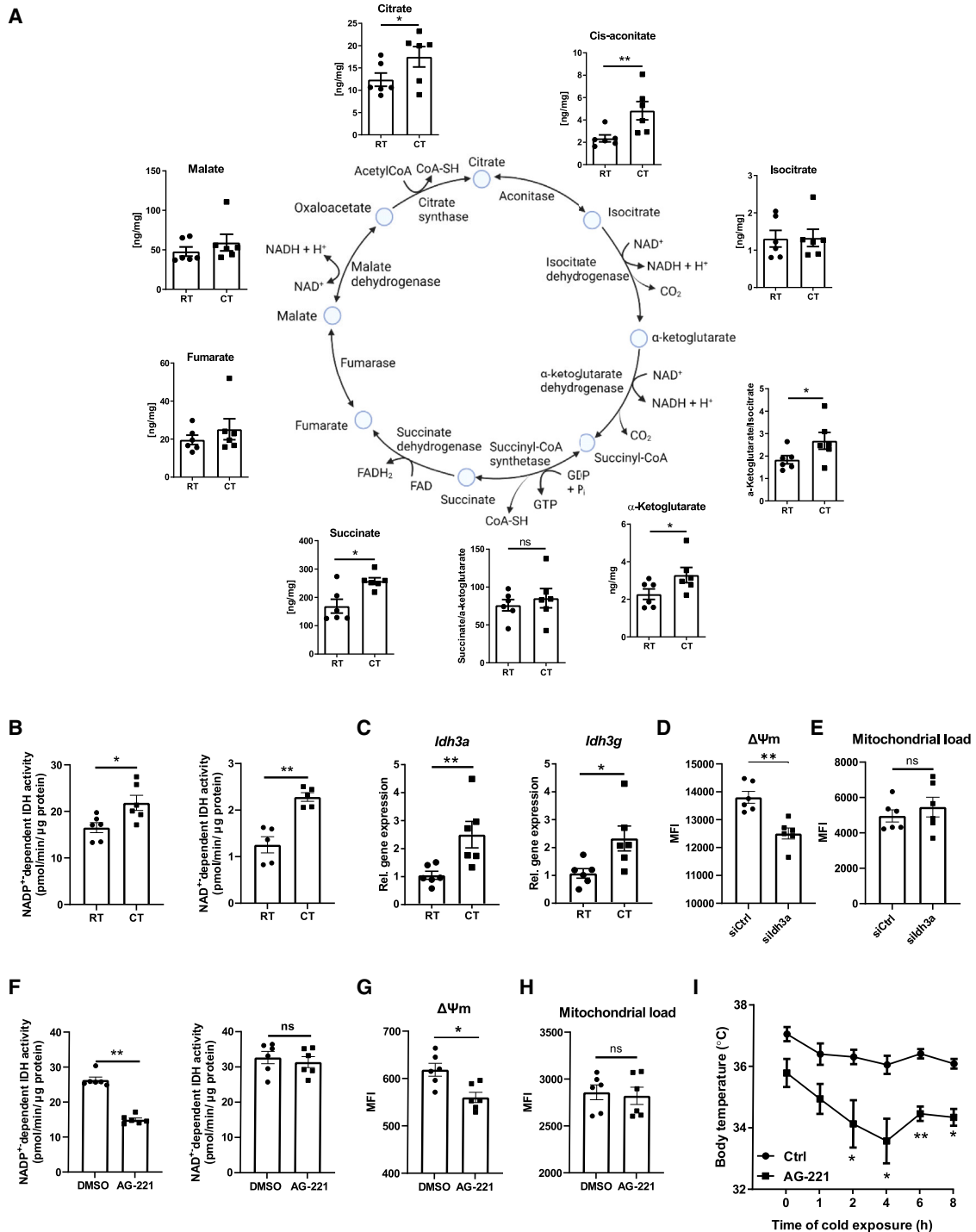


Figure 1. IDH promotes brown adipose tissue thermogenesis

(A) TCA cycle metabolite levels or ratios in BAT of WT mice kept for 8 h at 4°C (CT) or room temperature (RT, 22°C) measured by LC-MS/MS ($n = 6$ mice per group).

(B) NAD^+ and NAD^+ -dependent IDH activity normalized to protein concentration in BAT of WT mice kept for 8 h at CT or RT ($n = 6$ mice per group).

(C) Relative gene expression of *Idh3a* and *Idh3g* in BAT of mice kept for 8 h at CT or RT. Gene expression is set as 1 for RT samples ($n = 6$ mice per group).

(D and E) $\Delta\Psi\text{m}$ and mitochondrial load measured by TMRE and MitoTracker Green FM staining, respectively, and fluorescence-activated cell sorting (FACS) in brown preadipocytes (cell line) 48 h after transfection with siRNA against *Idh3a* or siCtrl ($n = 6$).

(legend continued on next page)

RESULTS

Isocitrate dehydrogenase is required for BAT thermogenesis

First, we asked whether TCA cycle activity in brown adipocytes plays a role in thermogenesis. To this end, we analyzed TCA cycle metabolite amounts by liquid chromatography-tandem mass spectrometry (LC-MS/MS) in BAT of C57BL/6N wild-type (WT) mice kept from birth at ambient temperature 22°C and at the age of 8–12 weeks exposed or not for 8 h to cold temperature (CT, 4°C). Cold exposure resulted in drop of body core temperature (Figure S1A) and increased *Ucp1* and *Pgc1a* mRNA and UCP1 protein expression in BAT (Figures S1B and S1C). Citrate, *cis*-aconitate, α -ketoglutarate and succinate amounts were upregulated in BAT of cold-exposed animals, while isocitrate, fumarate and malate levels remained unaltered (Figure 1A). The observed increase of α -ketoglutarate and succinate levels in BAT of mice upon cold exposure was in accordance with previous studies.^{11,20} While succinate is sequestered from the systemic circulation in BAT upon cold exposure, α -ketoglutarate is not.¹¹ Moreover, we observed an elevated α -ketoglutarate/isocitrate ratio indicating increased isocitrate dehydrogenase (IDH) activity in BAT of cold-exposed mice (Figure 1A). Confirming, NAD⁺ and NADP⁺-dependent IDH activity was elevated in BAT of cold-exposed mice (Figure 1B). In contrast, the succinate/ α -ketoglutarate ratio and α -ketoglutarate dehydrogenase (α -KGDH, oxoglutarate dehydrogenase [OGDH]) activity was not increased in BAT of cold-exposed mice (Figures 1A and S1D). Hence, IDH but not OGDH activity was upregulated by cold in BAT.

Three mammalian IDH isoforms exist. IDH1 (residing in the cytoplasm and peroxisomes) and IDH2 (residing in the mitochondrial matrix) catalyze the NADP⁺-dependent conversion of isocitrate to α -ketoglutarate; IDH3 catalyzes the NAD⁺-dependent conversion of isocitrate to α -ketoglutarate and localizes in the mitochondrial matrix.²¹ *Idh3a* and *Idh3g* expression was upregulated in BAT of cold-exposed mice (Figure 1C), standing in accordance with previous reports,²⁰ while *Idh1* and *Idh2* expression remained unchanged (Figure S1E). *Idh3a* silencing in brown preadipocytes (Figure S1F) reduced the $\Delta\Psi_m$, measured by Tetramethylrhodamine, ethyl ester (TMRE) staining (Figure 1D), without affecting the mitochondrial load, measured by MitoTracker Green FM staining (Figure 1E). However, *Idh3a* silencing or *Idh3a* overexpression or *Idh2* overexpression in brown preadipocytes did not alter *Ucp1* gene expression (Figures S1F–S1H). For IDH2 inhibition we used AG-221 (enasidenib), which although designed to inhibit mutant IDH2, was also reported to inhibit wild-type IDH2.²² Indeed, AG-221 decreased the NADP⁺-dependent IDH activity in brown adipocytes but did not affect the NAD⁺-dependent IDH activity (Figure 1F), indicating that AG-221 inhibits IDH2 but not IDH3. AG-221 decreased the $\Delta\Psi_m$ (Figure 1G) without affecting the mitochondrial load in brown adipocytes (Figure 1H). Accordingly, IDH2 overexpression in brown preadipocytes increased the $\Delta\Psi_m$ and

AG-221 diminished it (Figure S1I). In order to examine the impact of IDH2 inhibition on BAT thermogenesis, mice were treated by oral gavage with AG-221 and were then exposed for 8 h to cold. AG-221 treatment significantly decreased cold resistance of mice (Figure 1I) suggesting that IDH2 promotes cold-induced thermogenesis. Hence, IDH activity promotes $\Delta\Psi_m$ in brown adipocytes and cold resistance in mice.

In contrast, *Ogdh* silencing or overexpression did not alter the $\Delta\Psi_m$ in brown preadipocytes (Figures S1J and S1K). Moreover, inhibition of OGDH and pyruvate dehydrogenase (PDH) with CPI-613 did also not affect the $\Delta\Psi_m$ in brown adipocytes (Figure S1L).

These metabolic changes were specific for BAT, as levels of citrate, *cis*-aconitate, α -ketoglutarate and succinate were not altered upon cold exposure in inguinal subcutaneous adipose tissue (SAT), despite the fact that *Ucp1* and *Pgc1a* mRNA expression was increased, indicative for SAT “being” (Figures S2A and S2B). *Idh1* and *Idh2* expression and NADP⁺-dependent IDH activity remained unaltered while *Idh3a* expression increased upon cold exposure in SAT (Figures S2C and S2D). In gonadal adipose tissue (GAT), neither *Ucp1*, *Pgc1a*, *Idh1*, *Idh2*, and *Idh3a* mRNA expression nor the amounts of TCA cycle metabolites increased upon cold exposure (Figures S2E–S2G). Moreover, *Idh2*, *Idh3a*, *Idh3g*, and NAD⁺- and NADP⁺-dependent IDH activity remained unchanged upon cold exposure in gastrocnemius (Figures S3A and S3B) and quadriceps muscles (Figure S3C). These data collectively suggest that IDH activity is upregulated by cold in BAT, but not SAT, GAT, or skeletal muscle.

ADCY10, a bicarbonate sensor, promotes brown adipose tissue thermogenesis in a UCP1-independent manner

The IDH-dependent oxidative decarboxylation of isocitrate to α -ketoglutarate produces CO₂, which is transformed to bicarbonate by carbonic anhydrases (CA).¹³ We asked whether the TCA cycle-deriving CO₂/bicarbonate plays a role in brown adipocyte thermogenesis. CA inhibition by acetazolamide reduced the $\Delta\Psi_m$ in brown adipocytes (Figure 2A). In accordance, incubation of brown adipocytes in a CO₂ – free atmosphere (while maintaining the pH constant at 7.4) diminished the $\Delta\Psi_m$ (Figure 2B) and oxygen consumption rate (OCR) (Figure 2C) in brown adipocytes.

ADCY10 is a soluble adenylate cyclase residing in mitochondria and is activated by bicarbonate.¹⁷ We hypothesized that ADCY10 may sense IDH-generated CO₂/bicarbonate and support thermogenesis in brown adipocytes. Across different mouse organs and tissues, *Adcy10* was highly expressed in BAT, followed by SAT, GAT, and kidneys (Figures 2D and 2E). *Adcy10* expression in testes was much (1000-fold) higher compared to the here presented organs and for visualization reasons was not included in the graph. Upon cold exposure, *Adcy10* mRNA expression increased in BAT, but not SAT, GAT or skeletal (gastrocnemius, quadriceps) muscle (Figures 2E, S3A, and S3C). Whole-body ADCY10 deficient mice (Figure 2F), were engaged in cold

(F) NADP⁺ and NAD⁺-dependent IDH activity measured in brown adipocytes (cell line) treated for 18 h with 5 μ M AG-221 or same amount of DMSO ($n = 6$). (G and H) $\Delta\Psi_m$ and mitochondrial load in brown adipocytes (cell line) treated for 18 h with 5 μ M AG-221 or same amount of DMSO ($n = 6$). Mean fluorescence intensity (MFI) is shown in (D, E, G and H).

(I) Body temperature of mice pre-treated 2 h prior to cold exposure with 40 mg/kg AG-221 or control solution (0.5% methylcellulose/0.2% Tween 80% in water) and exposed for 8 h to 4°C ($n = 7$ –8 mice per group). All data are shown as mean \pm SEM. * $p < 0.05$, ** $p < 0.01$, ns: not significant.

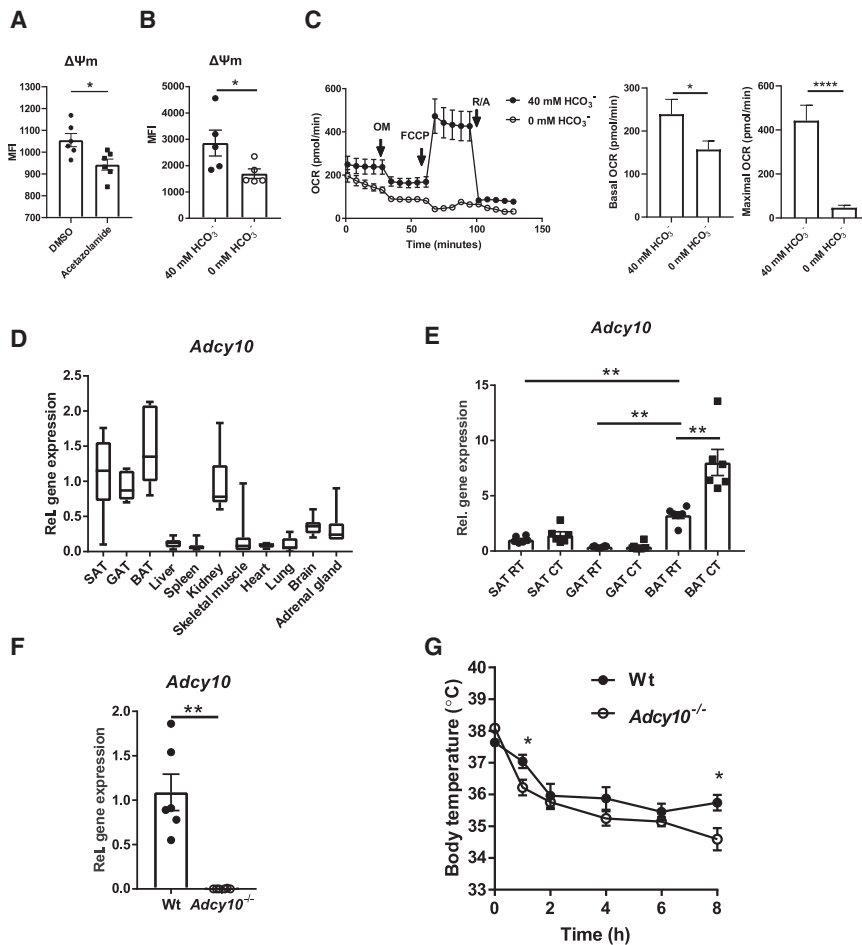


Figure 2. ADCY10 promotes thermogenesis in brown adipose tissue

(A) Brown adipocytes (cell line) were treated for 18 h with 1 mM acetazolamide or carrier (DMSO) and the $\Delta\Psi_m$ was measured by TMRE staining and FACS ($n = 6$).

(B) Primary brown adipocytes were kept for 24 h in a CO_2 -free atmosphere and the $\Delta\Psi_m$ was measured by TMRE staining ($n = 5$).

(C) The OCR was measured in primary brown adipocytes kept for 24 h in a CO_2 -free atmosphere (left). Quantification of basal and maximal OCR is shown (right) ($n = 15$). OM: oligomycin, R/A: rotenone/antimycin.

(D) *Adcy10* relative gene expression in different organs and tissues of WT mice ($n = 7$).

(E) *Adcy10* relative gene expression in subcutaneous (SAT), gonadal (GAT), and brown adipose tissue (BAT) in WT mice kept for 8 h at CT or RT ($n = 6$).

(F) *Adcy10* relative gene expression in BAT of WT and *Adcy10*^{-/-} mice; gene expression was set as 1 in WT mice ($n = 6$).

(G) Body temperature of WT and *Adcy10*^{-/-} mice exposed for 8 h to 4°C ($n = 10$ –14 mice per group). Data are shown as mean \pm SEM. * $p < 0.05$, ** $p < 0.01$, **** $p < 0.0001$.

ADCY10 maintains the mitochondrial membrane potential in brown adipocytes via EPAC1

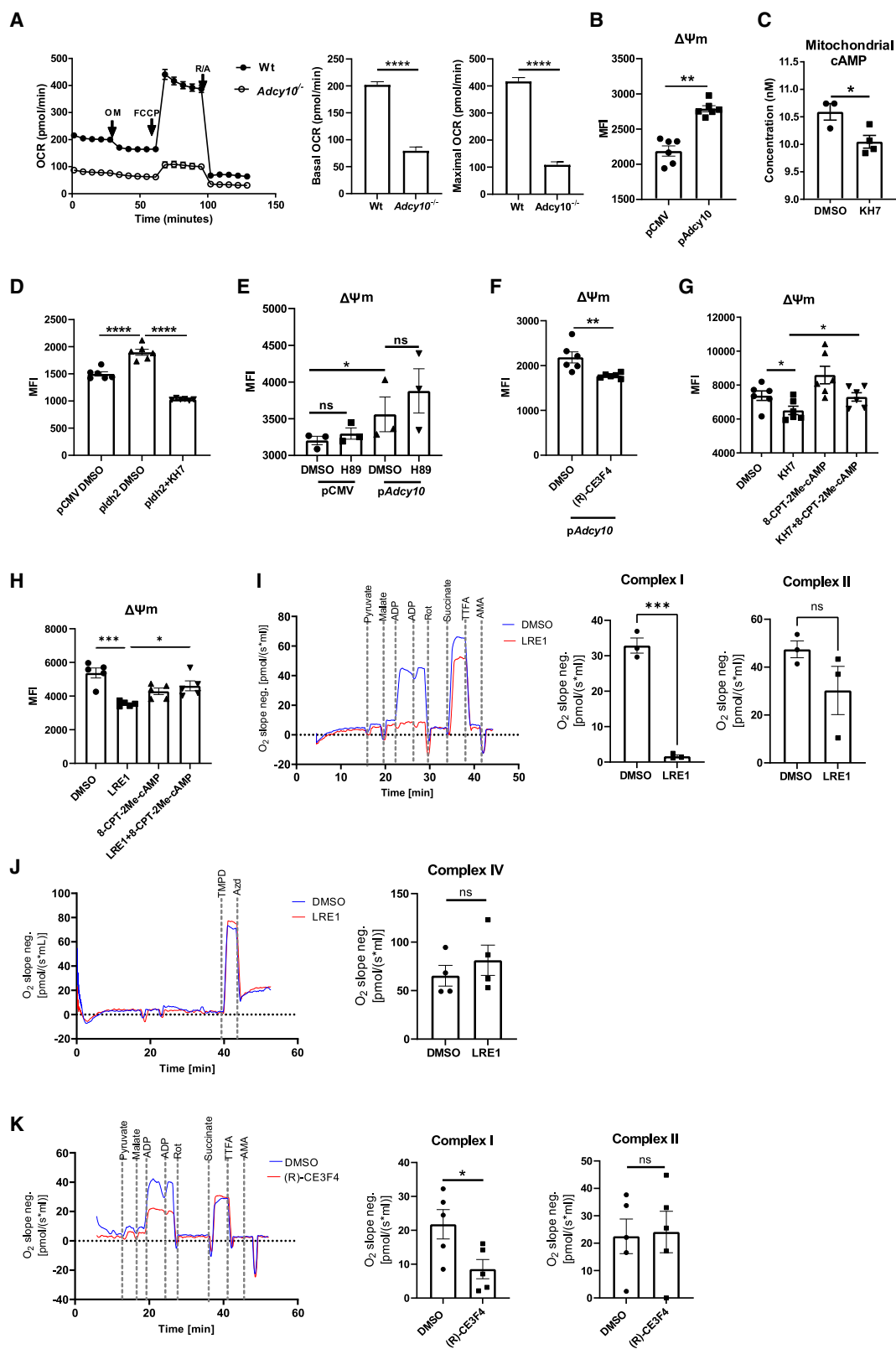
Next, we set out to dissect the mechanism mediating the effect of ADCY10 on BAT thermogenesis. Strikingly, OCR was strongly reduced in *Adcy10*^{-/-}

resistance studies, which showed that *Adcy10*^{-/-} mice exposed to 4°C were less cold resistant compared to WT littermate control mice (Figure 2G). However, ADCY10 deficiency did not affect UCP1 and PGC1A expression or the expression of other thermogenesis-related genes (*Prdm16* and *Cidea*), or the expression of subunits of ETC complexes in BAT of cold-exposed animals (Figures S4A–S4C). In accordance, basal and CL316,243-induced *Ucp1* and *Pgc1a* expression was not affected by ADCY10 deficiency in brown adipocytes (Figure S4D). ADCY10 overexpression also did not affect *Ucp1* expression in brown preadipocytes treated or not with the β_3 adrenergic receptor ligand isoproterenol (Figure S4E). In accordance, acetazolamide did not affect *Ucp1* expression in brown adipocytes treated with the β_3 adrenoceptor agonist CL316,243 (Figure S4F). Of note, there was no difference in the cell growth and adipogenic differentiation of brown adipocytes isolated from WT and *Adcy10*^{-/-} mice (Figures S4G and S4H). Moreover, ADCY10 deficiency did not alter the core body temperature, glucose tolerance or whole-body energy expenditure (EE) of mice kept at 22°C (Figures S4I–S4K). Together, these data demonstrate that ADCY10 is upregulated by cold specifically in BAT, but not SAT, GAT or skeletal muscle, and that its deficiency impairs cold resistance; however, without affecting UCP1 expression. Nevertheless, at normal ambient temperature (22°C) its role in whole body metabolism is negligible.

brown adipocytes compared to WT cells measured by Seahorse technology (Figure 3A), while ADCY10 overexpression increased the $\Delta\Psi_m$ in brown preadipocytes (Figure 3B). Moreover, the ADCY10 inhibitor KH7 reduced the mitochondrial cAMP amounts in WT but not *Adcy10*^{-/-} brown adipocytes, validating the inhibitory effect of KH7 on ADCY10 (Figures 3C and S4L). Mitochondrial isolation was confirmed by succinate dehydrogenase B (SDHB) positivity (Figure S4M). KH7 also blunted the increase in the $\Delta\Psi_m$, which was induced by *Idh2* overexpression (Figure 3D), suggesting that ADCY10 lies downstream of IDH2 in the regulation of the $\Delta\Psi_m$.

cAMP generated by ADCY10 may activate at least two distinct pathways, the PKA or the exchange protein activated by cAMP (EPAC1)-dependent pathway.^{13,17,18,23} While treatment with the PKA inhibitor H89 did not affect the $\Delta\Psi_m$ neither at basal conditions nor after ADCY10 overexpression (Figure 3E), EPAC1 inhibition by (R)-CE3F4 reduced the $\Delta\Psi_m$ in brown preadipocytes overexpressing ADCY10 (Figure 3F). In accordance, the membrane-permeable cAMP analogue 8-CPT-2Me-cAMP restored the $\Delta\Psi_m$ of brown adipocytes treated with the ADCY10 inhibitors KH7 or LRE1 (Figures 3G and 3H).

ADCY10 was reported to promote complex I and II activities.^{17,18,24,25} In brown adipocytes, ADCY10 inhibition by LRE1 reduced pyruvate and malate-driven complex I activity, as



(legend on next page)

assessed by high-resolution respirometry (Figure 3I). In contrast, succinate-driven complex II (SDH) or complex IV activity was not affected by LRE1 (Figures 3I and 3J). Similarly, the EPAC1 inhibitor (R)-CE3F4 decreased complex I but not complex II activity (Figure 3K). Hence, we suggest that ADCY10 through EPAC1 increases complex I activity, which sustains the $\Delta\Psi_m$ in brown adipocytes, thereby allowing UCP1 function and thermogenesis.

DISCUSSION

BAT thermogenesis counters metabolic disease.^{5–7} It is mediated by uncoupling of oxidative phosphorylation via UCP1, the function of which relies on the efficiency of the ETC to maintain the $\Delta\Psi_m$.²⁶ Although regulation of UCP1 expression by the nervous, endocrine or immune systems has been extensively studied,^{5,6,27} less is known about the mechanisms sustaining the $\Delta\Psi_m$ in brown adipocytes. Here, we report a cell metabolic mechanism, which maintains the $\Delta\Psi_m$ in brown adipocytes and promotes thermogenesis. We show that upon cold exposure, IDH activity and the expression of the soluble adenylate cyclase (ADCY10) are upregulated in BAT of mice. This effect is specific for BAT and is not observed in SAT, GAT or skeletal muscle. Moreover, IDH inhibition or ADCY10 deficiency reduce cold resistance in mice, interestingly, without affecting UCP1 expression in BAT. Instead, our *in vitro* experiments in primary brown adipocytes and a brown adipocyte cell line suggest that the IDH-ADCY10 axis sustains the $\Delta\Psi_m$ in brown adipocytes thereby allowing efficient thermogenesis.

In contrast to tmAC, ADCY10 localizes in different subcellular compartments, including mitochondria.¹² Specifically, according to a recent study in cardiomyocytes, ADCY10 likely localizes in the intermembrane space (IMS) of mitochondria.¹³ Previous studies showed that mitochondrial ADCY10 functions as a bicarbonate sensor and generates cAMP, a second messenger, which signals promoting ETC function and concomitant ATP production.^{17–19} We propose that in brown adipocytes CO₂/bicarbonate generated by IDH activity may activate ADCY10, which produces cAMP in mitochondria. The latter sustains the $\Delta\Psi_m$ through EPAC1 activation thereby facilitating the function of UCP1. Our data together with data of previous studies in other cell types sug-

gest that mitochondrial ADCY10 via positive regulation of ETC function may promote either thermogenesis or ATP production depending on the cell type and UCP1 expression levels: low UCP1 expression allowing high ATP production as in hepatocytes¹⁷ or cardiomyocytes,¹³ while high UCP1 expression mediating thermogenesis, as shown here in brown adipocytes.

Interestingly, although CO₂ in mitochondria derives from decarboxylation of different TCA-linked metabolites, that is pyruvate, α -ketoglutarate and isocitrate, only isocitrate decarboxylation was found to be coupled to increased $\Delta\Psi_m$ and thermogenesis in brown adipocytes. The reason underlying this specificity for mitochondrial IDH activity remains unclear. However, our findings stand in accordance with reports in *D. melanogaster* showing that IDH activity is required for oxidative phosphorylation in myocytes.²⁸ Accordingly, IDH2 deficient mice have reduced mitochondrial function and BAT activity and gain more weight when fed a high-fat diet.²⁹ Moreover, α -ketoglutarate was shown to be required for active DNA demethylation of the *Prdm16* promoter in brown adipocytes thereby promoting brown adipogenesis.³⁰ On the contrary, IDH1, the cytoplasmic IDH isoform, was reported to inhibit brown adipogenesis.³¹

ADCY10 was shown to mediate its effects in mitochondria via cAMP coupled to either PKA^{17,19} or EPAC1 signaling.^{13,18,32} We demonstrate that in brown adipocytes the effect of ADCY10 on the $\Delta\Psi_m$ is mediated by EPAC1 and not PKA. Moreover, similarly to previous reports, we found that the ADCY10-EPAC1 axis promotes complex I activity without affecting complex II or IV activities.^{18,24} In conclusion, we suggest that the IDH-CO₂/bicarbonate-ADCY10-EPAC1-complex I axis is essential for maintaining the $\Delta\Psi_m$ in brown adipocytes thereby enabling UCP1 function and efficient thermogenesis. These findings reveal a novel regulatory mechanism of BAT function and may be valuable in the pathophysiology and management of metabolic disease.

Limitations of the study

In summary, we show that IDH and ADCY10 regulate BAT thermogenesis via sustaining the $\Delta\Psi_m$ in brown adipocytes. A limitation of the study is that the significance of this mechanism was not studied in the context of obesity and metabolic disease.

Figure 3. ADCY10 maintains the mitochondrial membrane potential via cAMP-EPAC1

- (A) OCR measured in WT and *Adcy10*^{-/-} primary brown adipocytes (left) and quantification of basal and maximal OCR (right) (*n* = 12).
 (B) Brown preadipocytes were plasmid transfected to overexpress ADCY10 and 48 h later the $\Delta\Psi_m$ was measured by TMRE staining and FACS (*n* = 6).
 (C) Brown adipocytes (cell line) were treated for 2 h with 10 μ M KH7 and cAMP was measured in isolated mitochondria (*n* = 3–4).
 (D) Brown preadipocytes (cell line) were transfected with *Idh2*-overexpressing plasmid or control plasmid for 48 h and treated with 10 μ M KH7 or control carrier (DMSO) for 2 h; the $\Delta\Psi_m$ was measured by TMRE staining and FACS (*n* = 6).
 (E) Brown preadipocytes (cell line) were transfected with an ADCY10-overexpressing or a control plasmid for 48 h and treated the last 24 h with 10 μ M H89 or DMSO; the $\Delta\Psi_m$ was measured by TMRE staining and FACS (*n* = 3).
 (F) Brown preadipocytes were plasmid transfected for 48 h to overexpress ADCY10 and treated for 2 h with 10 μ M (R)-CE3F4 or DMSO. The $\Delta\Psi_m$ was measured by TMRE staining and FACS (*n* = 6).
 (G and H) Brown adipocytes (cell line) were treated for 18 h with 10 μ M KH7 or 50 μ M LRE1 or DMSO and 100 μ M 8-CPT-2Me-cAMP or PBS and the $\Delta\Psi_m$ was measured by TMRE staining and FACS (*n* = 5–6).
 (I and K) Brown adipocytes (cell line) were treated for 2 h with 50 μ M LRE1, 10 μ M (R)-CE3F4 or DMSO and complex I and II activity was measured by high-resolution respirometry by sequential addition of 5 mM pyruvate, 2 mM malate, 5 mM ADP⁺Mg²⁺, 0.5 μ M rotenone, 10 mM succinate, 12.5 μ M thenoyltrifluoroacetone (TTFA) and 2.5 μ M antimycin (AMA) (*n* = 3–5).
 (J) Brown adipocytes (cell line) were treated for 2 h with 50 μ M LRE1 and complex IV activity was measured by high-resolution respirometry by addition of 0.5 mM tetramethyl-*p*-phenylenediamine (TMPD) and 40 mM sodium azide (Azd) (*n* = 4). Data are shown as mean \pm SEM. **p* < 0.05, ***p* < 0.01, ****p* < 0.001, ns: not significant.

Moreover, we did not study the relevance of this mechanism in human BAT.

RESOURCE AVAILABILITY

Lead contact

Requests for further information and resources should be directed to and will be fulfilled by the lead contact, Vasileia Ismini Alexaki (Institute for Clinical Chemistry and Laboratory Medicine, Faculty of Medicine, University Clinic Carl Gustav Carus, Technische Universität Dresden, Fetscherstrasse 74, Dresden, 01307, Germany, tel. +4935145816273, Vasileialsmini.Alexaki@uniklinikum-dresden.de).

Material availability statement

The study did not generate new unique reagents.

Data and code availability

- All data presented in the study will be shared by the [lead contact](#) upon request.
- This paper does not report original code.
- Any additional information required to reanalyze the data reported in this paper is available from the [lead contact](#) upon request.

ACKNOWLEDGMENTS

We thank Yuri Ladilov (Department of Cardiovascular Surgery, Heart Center Brandenburg, Brandenburg Medical School, Bernau bei Berlin, Germany) for providing the *Adcy10*^{-/-} mice. We also thank Matthias Blüher (Clinic and Policlinic for Endocrinology and Nephrology, Medical Research Center, Universitätsmedizin Leipzig, Germany) for providing the brown adipocyte cell line. Finally, we thank the Experimental Mass Spectrometry Unit from the Institute of Clinical Chemistry and Laboratory Medicine, and Carmen Hentsche (Department of Physiology, Faculty of Medicine, Technische Universität Dresden) for technical assistance. This work was supported by grants from the Deutsche Forschungsgemeinschaft (AL 1686/6-1 and SFB-TRR 205, project A7 to V.I.A. and SFB-TRR 127, project A3 to T.C.), and the Saxon State Ministry of Science, Culture and Tourism-SMWK (Unterstützung profilbestimmender Struktureinheiten der TU Dresden, to T.C.).

AUTHOR CONTRIBUTIONS

A.Das, methodology, validation, formal analysis, investigation; C.M., methodology, investigation; E.H., investigation; R.G.-M., investigation; E.K., investigation; A.W., investigation; M.P., investigation; A.Deussen, resources; T.C., resources, conceptualization; T.N., resources, conceptualization; V.I.A., conceptualization, resources, writing – original draft, writing – review & editing, visualization, supervision, project administration, funding acquisition.

DECLARATION OF INTERESTS

The authors declare no competing interests.

STAR★METHODS

Detailed methods are provided in the online version of this paper and include the following:

- [KEY RESOURCES TABLE](#)
- [EXPERIMENTAL MODEL AND STUDY PARTICIPANT DETAILS](#)
- [METHOD DETAILS](#)
 - Cell transfections and treatments
 - Measurement of tricarboxylic acid cycle metabolites
 - Isolation of mitochondria
 - cAMP measurement
 - Enzyme activity measurement
 - Seahorse analysis
 - High-resolution respirometry

- Mitochondrial load and membrane potential assessment
- Cell growth assessment
- Oil Red O staining
- Western blot
- Quantitative RT – PCR

● QUANTIFICATION AND STATISTICAL ANALYSIS

SUPPLEMENTAL INFORMATION

Supplemental information can be found online at <https://doi.org/10.1016/j.isci.2025.111833>.

Received: May 2, 2024

Revised: November 1, 2024

Accepted: January 15, 2025

Published: January 19, 2025

REFERENCES

1. Chouchani, E.T., Kazak, L., and Spiegelman, B.M. (2019). New Advances in Adaptive Thermogenesis: UCP1 and Beyond. *Cell Metabol.* 29, 27–37. <https://doi.org/10.1016/j.cmet.2018.11.002>.
2. Harms, M., and Seale, P. (2013). Brown and beige fat: development, function and therapeutic potential. *Nat. Med.* 19, 1252–1263. <https://doi.org/10.1038/nm.3361>.
3. Bertholet, A.M., and Kirichok, Y. (2017). UCP1: A transporter for H(+) and fatty acid anions. *Biochimie* 134, 28–34. <https://doi.org/10.1016/j.biochi.2016.10.013>.
4. Liu, X., Zhang, Z., Song, Y., Xie, H., and Dong, M. (2022). An update on brown adipose tissue and obesity intervention: Function, regulation and therapeutic implications. *Front. Endocrinol.* 13, 1065263. <https://doi.org/10.3389/fendo.2022.1065263>.
5. Kajimura, S., Spiegelman, B.M., and Seale, P. (2015). Brown and Beige Fat: Physiological Roles beyond Heat Generation. *Cell Metabol.* 22, 546–559. <https://doi.org/10.1016/j.cmet.2015.09.007>.
6. Carpentier, A.C., Blondin, D.P., Haman, F., and Richard, D. (2023). Brown Adipose Tissue-A Translational Perspective. *Endocr. Rev.* 44, 143–192. <https://doi.org/10.1210/endrev/bnac015>.
7. Whittle, A.J., López, M., and Vidal-Puig, A. (2011). Using brown adipose tissue to treat obesity - the central issue. *Trends Mol. Med.* 17, 405–411. <https://doi.org/10.1016/j.molmed.2011.04.001>.
8. Cypess, A.M., Lehman, S., Williams, G., Tal, I., Rodman, D., Goldfine, A.B., Kuo, F.C., Palmer, E.L., Tseng, Y.H., Doria, A., et al. (2009). Identification and importance of brown adipose tissue in adult humans. *N. Engl. J. Med.* 360, 1509–1517. <https://doi.org/10.1056/NEJMoa0810780>.
9. van Marken Lichtenbelt, W.D., Vanhommel, J.W., Smulders, N.M., Drossaerts, J.M.A.F.L., Kemerink, G.J., Bouvy, N.D., Schrauwen, P., and Teule, G.J.J. (2009). Cold-activated brown adipose tissue in healthy men. *N. Engl. J. Med.* 360, 1500–1508. <https://doi.org/10.1056/NEJMoa0808718>.
10. Hanssen, M.J.W., van der Lans, A.A.J.J., Brans, B., Hoeks, J., Jardon, K.M.C., Schaart, G., Mottaghy, F.M., Schrauwen, P., and van Marken Lichtenbelt, W.D. (2016). Short-term Cold Acclimation Recruits Brown Adipose Tissue in Obese Humans. *Diabetes* 65, 1179–1189. <https://doi.org/10.2337/db15-1372>.
11. Mills, E.L., Pierce, K.A., Jedrychowski, M.P., Garrity, R., Winther, S., Vidoni, S., Yoneshiro, T., Spinelli, J.B., Lu, G.Z., Kazak, L., et al. (2018). Accumulation of succinate controls activation of adipose tissue thermogenesis. *Nature* 560, 102–106. <https://doi.org/10.1038/s41586-018-0353-2>.
12. Zippin, J.H., Chen, Y., Nahimey, P., Kamenetsky, M., Wuttke, M.S., Fischman, D.A., Levin, L.R., and Buck, J. (2003). Compartmentalization of bicarbonate-sensitive adenylyl cyclase in distinct signaling microdomains. *FASEB J.* 17, 82–84. <https://doi.org/10.1096/fj.02-0598fj>.
13. Greiser, M., Karbowski, M., Kaplan, A.D., Coleman, A.K., Verhoeven, N., Mannella, C.A., Lederer, W.J., and Boyman, L. (2023). Calcium and

- bicarbonate signaling pathways have pivotal, resonating roles in matching ATP production to demand. *Elife* 12, e84204. <https://doi.org/10.7554/eLife.84204>.
14. Buck, J., Sinclair, M.L., Schapal, L., Cann, M.J., and Levin, L.R. (1999). Cytosolic adenylyl cyclase defines a unique signaling molecule in mammals. *Proc. Natl. Acad. Sci. USA* 96, 79–84. <https://doi.org/10.1073/pnas.96.1.79>.
 15. Litvin, T.N., Kamenetsky, M., Zarifyan, A., Buck, J., and Levin, L.R. (2003). Kinetic properties of "soluble" adenylyl cyclase. Synergism between calcium and bicarbonate. *J. Biol. Chem.* 278, 15922–15926. <https://doi.org/10.1074/jbc.M212475200>.
 16. Rossetti, T., Jackvony, S., Buck, J., and Levin, L.R. (2021). Bicarbonate, carbon dioxide and pH sensing via mammalian bicarbonate-regulated soluble adenylyl cyclase. *Interface Focus* 11, 20200034. <https://doi.org/10.1098/rsfs.2020.0034>.
 17. Acin-Perez, R., Salazar, E., Kamenetsky, M., Buck, J., Levin, L.R., and Manfredi, G. (2009). Cyclic AMP produced inside mitochondria regulates oxidative phosphorylation. *Cell Metabol.* 9, 265–276. <https://doi.org/10.1016/j.cmet.2009.01.012>.
 18. Chang, J.C., Go, S., Giglioni, E.H., Duijst, S., Panneman, D.M., Rodenburg, R.J., Li, H.L., Huang, H.L., Levin, L.R., Buck, J., et al. (2021). Soluble adenylyl cyclase regulates the cytosolic NADH/NAD(+) redox state and the bioenergetic switch between glycolysis and oxidative phosphorylation. *Biochim. Biophys. Acta Bioenerg.* 1862, 148367. <https://doi.org/10.1016/j.bbabi.2020.148367>.
 19. Di Benedetto, G., Scalzotto, E., Mongillo, M., and Pozzan, T. (2013). Mitochondrial Ca²⁺(+) uptake induces cyclic AMP generation in the matrix and modulates organelle ATP levels. *Cell Metabol.* 17, 965–975. <https://doi.org/10.1016/j.cmet.2013.05.003>.
 20. Jung, S.M., Doxsey, W.G., Le, J., Haley, J.A., Mazuecos, L., Luciano, A.K., Li, H., Jang, C., and Guertin, D.A. (2021). In vivo isotope tracing reveals the versatility of glucose as a brown adipose tissue substrate. *Cell Rep.* 36, 109459. <https://doi.org/10.1016/j.celrep.2021.109459>.
 21. Al-Khallaif, H. (2017). Isocitrate dehydrogenases in physiology and cancer: biochemical and molecular insight. *Cell Biosci.* 7, 37. <https://doi.org/10.1186/s13578-017-0165-3>.
 22. Jaccard, A., Wyss, T., Maldonado-Pérez, N., Rath, J.A., Bevilacqua, A., Peng, J.J., Lepez, A., Von Gunten, C., Franco, F., Kao, K.C., et al. (2023). Reductive carboxylation epigenetically instructs T cell differentiation. *Nature* 621, 849–856. <https://doi.org/10.1038/s41586-023-06546-y>.
 23. Szanda, G., Wisniewski, É., Rajki, A., and Spät, A. (2018). Mitochondrial cAMP exerts positive feedback on mitochondrial Ca²⁺ uptake via the recruitment of Epac1. *J. Cell Sci.* 131, jcs215178. <https://doi.org/10.1242/jcs.215178>.
 24. De Rasmio, D., Signorile, A., Santeramo, A., Larizza, M., Lattanzio, P., Capitano, G., and Papa, S. (2015). Intramitochondrial adenylyl cyclase controls the turnover of nuclear-encoded subunits and activity of mammalian complex I of the respiratory chain. *Biochim. Biophys. Acta* 1853, 183–191. <https://doi.org/10.1016/j.bbamcr.2014.10.016>.
 25. De Rasmio, D., Micelli, L., Santeramo, A., Signorile, A., Lattanzio, P., and Papa, S. (2016). cAMP regulates the functional activity, coupling efficiency and structural organization of mammalian FOF1 ATP synthase. *Biochim. Biophys. Acta* 1857, 350–358. <https://doi.org/10.1016/j.bbabi.2016.01.006>.
 26. Chouchani, E.T., Kazak, L., and Spiegelman, B.M. (2017). Mitochondrial reactive oxygen species and adipose tissue thermogenesis: Bridging physiology and mechanisms. *J. Biol. Chem.* 292, 16810–16816. <https://doi.org/10.1074/jbc.R117.789628>.
 27. Alexaki, V.I., and Chavakis, T. (2016). The role of innate immunity in the regulation of brown and beige adipogenesis. *Rev. Endocr. Metab. Disord.* 17, 41–49. <https://doi.org/10.1007/s11154-016-9342-7>.
 28. Murari, A., Goparaju, N.S.V., Rhooms, S.K., Hossain, K.F.B., Liang, F.G., Garcia, C.J., Osei, C., Liu, T., Li, H., Kitsis, R.N., et al. (2022). IDH2-mediated regulation of the biogenesis of the oxidative phosphorylation system. *Sci. Adv.* 8, eabl8716. <https://doi.org/10.1126/sciadv.abl8716>.
 29. Lee, J.H., Go, Y., Kim, D.Y., Lee, S.H., Kim, O.H., Jeon, Y.H., Kwon, T.K., Bae, J.H., Song, D.K., Rhyu, I.J., et al. (2020). Isocitrate dehydrogenase 2 protects mice from high-fat diet-induced metabolic stress by limiting oxidative damage to the mitochondria from brown adipose tissue. *Exp. Mol. Med.* 52, 238–252. <https://doi.org/10.1038/s12276-020-0379-z>.
 30. Yang, Q., Liang, X., Sun, X., Zhang, L., Fu, X., Rogers, C.J., Berim, A., Zhang, S., Wang, S., Wang, B., et al. (2016). AMPK/alpha-Ketoglutarate Axis Dynamically Mediates DNA Demethylation in the Prdm16 Promoter and Brown Adipogenesis. *Cell Metabol.* 24, 542–554. <https://doi.org/10.1016/j.cmet.2016.08.010>.
 31. Kang, H.S., Lee, J.H., Oh, K.J., Lee, E.W., Han, B.S., Park, K.Y., Suh, J.M., Min, J.K., Chi, S.W., Lee, S.C., et al. (2020). IDH1-dependent alpha-KG regulates brown fat differentiation and function by modulating histone methylation. *Metabolism* 105, 154173. <https://doi.org/10.1016/j.metabol.2020.154173>.
 32. Wang, Z., Liu, D., Varin, A., Nicolas, V., Courilleau, D., Mateo, P., Caubere, C., Rouet, P., Gomez, A.M., Vandecasteele, G., et al. (2016). A cardiac mitochondrial cAMP signaling pathway regulates calcium accumulation, permeability transition and cell death. *Cell Death Dis.* 7, e2198. <https://doi.org/10.1038/cddis.2016.106>.
 33. Fasshauer, M., Klein, J., Ueki, K., Kriauciunas, K.M., Benito, M., White, M.F., and Kahn, C.R. (2000). Essential role of insulin receptor substrate-2 in insulin stimulation of Glut4 translocation and glucose uptake in brown adipocytes. *J. Biol. Chem.* 275, 25494–25501. <https://doi.org/10.1074/jbc.M004046200>.
 34. Esposito, G., Jaiswal, B.S., Xie, F., Krajnc-Franken, M.A.M., Robben, T.J.A.A., Strik, A.M., Kuil, C., Philipsen, R.L.A., van Duin, M., Conti, M., and Gossen, J.A. (2004). Mice deficient for soluble adenylyl cyclase are infertile because of a severe sperm-motility defect. *Proc. Natl. Acad. Sci. USA* 101, 2993–2998. <https://doi.org/10.1073/pnas.0400050101>.
 35. Schindelin, J., Arganda-Carreras, I., Frise, E., Kaynig, V., Longair, M., Pietzsch, T., Preibisch, S., Rueden, C., Saalfeld, S., Schmid, B., et al. (2012). Fiji: an open-source platform for biological-image analysis. *Nat. Methods* 9, 676–682. <https://doi.org/10.1038/nmeth.2019>.
 36. Garcia-Martin, R., Alexaki, V.I., Qin, N., Rubin de Celis, M.F., Economopoulou, M., Ziogas, A., Gercken, B., Kotlabova, K., Phieler, J., Ehrhart-Bornstein, M., et al. (2016). Adipocyte-Specific Hypoxia-Inducible Factor 2alpha Deficiency Exacerbates Obesity-Induced Brown Adipose Tissue Dysfunction and Metabolic Dysregulation. *Mol. Cell Biol.* 36, 376–393. <https://doi.org/10.1128/MCB.00430-15>.
 37. Mateska, I., Witt, A., Hagag, E., Sinha, A., Yilmaz, C., Thanou, E., Sun, N., Kolliniati, O., Patschin, M., Abdelmegeed, H., et al. (2023). Succinate mediates inflammation-induced adrenocortical dysfunction. *Elife* 12, e83064. <https://doi.org/10.7554/eLife.83064>.
 38. Richter, S., Gieldon, L., Pang, Y., Peitzsch, M., Huynh, T., Leton, R., Viana, B., Ercolino, T., Mangelis, A., Rapizzi, E., et al. (2019). Metabolome-guided genomics to identify pathogenic variants in isocitrate dehydrogenase, fumarate hydratase, and succinate dehydrogenase genes in pheochromocytoma and paraganglioma. *Genet. Med.* 21, 705–717. <https://doi.org/10.1038/s41436-018-0106-5>.
 39. Witt, A., Mateska, I., Palladini, A., Sinha, A., Wölk, M., Harauma, A., Bechmann, N., Pamporaki, C., Dahl, A., Rothe, M., et al. (2023). Fatty acid desaturase 2 determines the lipidomic landscape and steroidogenic function of the adrenal gland. *Sci. Adv.* 9, eadf6710. <https://doi.org/10.1126/sciadv.adf6710>.

STAR★METHODS

KEY RESOURCES TABLE

REAGENT or RESOURCE	SOURCE	IDENTIFIER
Antibodies		
anti-UCP1	Abcam	ab10983; RRID: AB_2241462
anti-PGC1A	Merck Millipore	AB3242
Total OXPHOS Rodent WB Antibody Cocktail	Abcam	ab110413; RRID: AB_2629281
anti-SDHB	Sigma-Aldrich	HPA002868; RRID: AB_1079889
Anti-Vinculin	Santa Cruz Biotechnology	sc-25336; RRID: AB_628438
anti- β -Actin	Cell Signaling	#4970
Chemicals, peptides, and recombinant proteins		
AG-221, Enasidenib	Selleckchem	S8205
D-(+)-glucose	Sigma-Aldrich	G8270
Collagenase type I	Thermo Fisher Scientific	17100017
DMEM, high glucose, GlutaMAX™ Supplement, pyruvate	Thermo Fisher Scientific	31966021
Fetal Bovine Serum (FBS)	Thermo Fisher Scientific	10270106
Triiodothyronine (T3)	Sigma-Aldrich	642511
Insulin	Sigma-Aldrich	I5500
Isobutylmethylxanthine (IBMX)	Sigma-Aldrich	I5879
Dexamethasone	Sigma-Aldrich	D4902
Indomethacin	Sigma-Aldrich	I7378
Lipofectamine RNAiMAX transfection reagent	Thermo Fisher Scientific	13778150
Lipofectamine LTX Reagent	Thermo Fisher Scientific	15338100
Acetazolamide	Sigma-Aldrich	A6011
KH7	MedChemExpress	HY-103194
LRE1	MedChemExpress	HY-100524
(R)-CE3F4	MedChemExpress	HY-108539A
8-CPT-2Me-cAMP	Tocris	1645
CPI-613	Cayman Chemical	16981
CL316,243	MedChemExpress	HY-116771A
Isoproterenol	Sigma-Aldrich	I6504
H89	Selleckchem	S1582
Digitonin	Sigma-Aldrich	D5628
Malate	Sigma-Aldrich	M1000
Pyruvate	Sigma-Aldrich	P2256
Succinate	Sigma-Aldrich	S2378
Rotenone	Sigma-Aldrich	R8875
Thenoyltrifluoroacetone (TTFA)	Sigma-Aldrich	T27006
Antimycin	Sigma-Aldrich	A8674
Tetramethyl- <i>p</i> -phenylenediamine (TMPD)	Sigma-Aldrich	T3134
Ascorbate	Sigma-Aldrich	A4544
Sodium azide	Sigma-Aldrich	S2002
MitoTracker™ Green FM	Thermo Fisher Scientific	M46750
TMRE	Thermo Fisher Scientific	T669
PrestoBlue™ Cell Viability Reagent	Thermo Fisher Scientific	A13261
Oil Red O dye	Sigma-Aldrich	1024190250
Critical commercial assays		
cAMP Assay kit	Abcam	ab138880

(Continued on next page)

Continued

REAGENT or RESOURCE	SOURCE	IDENTIFIER
IDH Assay kit	Abcam	ab102528
OGDH Activity Assay kit	Biomol	G-MAES0236.96
Seahorse XF Cell Mito Stress Test Kit	Agilent	103015-100
Experimental models: Cell lines		
Mouse brown adipocyte cell line	Fasshauer et al., 2000 ³³	
Experimental models: Organisms/strains		
<i>Adcy10</i> ^{-/-} mice	Esposito et al., 2004 ³⁴	provided by Matthias Blüher (University of Leipzig, Germany)
C57BL/6N mice	Charles River	C57BL/6NCrl
Oligonucleotides		
TARGETplus SMARTpool siRNA against <i>Idh3a</i>	Horizon Discovery	L-061019-01-0005
TARGETplus SMARTpool siRNA against <i>Ogdh</i>	Horizon Discovery	L-044219-01-0005
Recombinant DNA		
<i>Idh2</i> (NM_173011) Mouse Tagged ORF Clone	Origene	MR207208
<i>Idh3a</i> (NM_029573) Mouse Tagged ORF Clone	Origene	MR205632
<i>Adcy10</i> (NM_173029) Mouse Tagged ORF Clone	Origene	MR217736
<i>Ogdh</i> (NM_010956) Mouse Untagged Clone	Origene	MC201038
Software		
TSE Phenomaster V7.7.9	TSE-Systems	https://www.tse-systems.com/
Synergy HT, Gen5 3.13	Agilent Technologies, Biotek	https://www.agilent.com/
Wave 2.6.3.5	Agilent Technologies, Seahorse	https://www.agilent.com/
DatLab 7.4.0.4	Oroboros Instruments	https://www.orooboros.at/
BD FACSDiva Software v. 6.1.3	BD Biosciences	https://www.bdbiosciences.com/
Fiji	Schindelin et al., 2012 ³⁵	https://www.nature.com/articles/nmeth.2019/
Bio-Rad CFX Manager v. 3.1	Bio-Rad	https://www.bio-rad.com/
GraphPrism 7.04	GraphPrism	https://www.graphpad.com/
Biorender	Biorender	https://www.biorender.com/

EXPERIMENTAL MODEL AND STUDY PARTICIPANT DETAILS

The mice were kept from birth at an ambient temperature of 22°C in standard housing conditions. Littermates of the same sex were randomly assigned to experimental groups. Mice with whole-body ADCY10 deficiency (*Adcy10*^{-/-}) were previously developed.³⁴ Cold exposure experiments were performed as previously described.³⁶ Ten-week-old male *Adcy10*^{-/-} mice or wt littermates or wt C57BL/6N mice (purchased from Charles River) were kept for 8 h at 4°C during the dark cycle of the mice with free access to water and food. In some experiments mice were treated with 40 mg/kg AG-221 (Enasidenib, from Selleckchem, diluted in 0.5% methylcellulose/0.2% Tween 80% in water) or control solution (0.5% methylcellulose/0.2% Tween 80% in water) through oral gavage 2 h before cold exposure. The body temperature was measured rectally before and during cold exposure at the indicated time points. Mice were killed by cervical dislocation, tissues were harvested, snap-frozen in liquid nitrogen and stored at -80°C for further analysis. For the glucose tolerance test, mice were fasted overnight and intraperitoneally injected with D-(+)-glucose (Sigma-Aldrich) (1 g/kg). Glucose was measured via the tail vein with an Accu-Chek glucometer (Roche) at 0, 15, 30, 60, 90 and 120 min.³⁶ In other experiments, mice were analyzed in metabolic cages (PhenoMaster; TSE Systems, Bad Homburg, Germany).³⁶ Volume of oxygen consumption (VO₂) and carbon dioxide production (VCO₂) were determined every 20 min. EE was calculated as (3.941 × VO₂) + (1.106 × VCO₂). All animal experiments were approved by the Landesdirektion Sachsen Germany (TVV57/2018, TVV67/2023).

Primary brown adipocytes were isolated from BAT of 3 weeks-old wt and *Adcy10*^{-/-} mice. BAT was chopped and digested for 1 h at 37°C in 2 mg/mL collagenase type I (Gibco) diluted in DMEM (Gibco) + 4% BSA (Sigma-Aldrich) under rigorous shaking. Then, samples were passed through a cell strainer (100 μm pore size) and centrifuged for 5 min at 200 g. Cells were washed with DMEM +4% BSA, centrifuged again for 5 min at 200 g, resuspended in growth medium (high-glucose DMEM, supplemented with GlutaMAX+ 20% Fetal Bovine Serum (FBS) (Gibco) 1% penicillin/streptomycin (Gibco)) and cultured in 35 mm-diameter dishes.

The used mouse brown adipocyte cell line, described previously,³³ was kindly provided by Matthias Blüher (University of Leipzig, Germany). Cells were cultured in high-glucose DMEM, supplemented with GlutaMAX+ 20% FBS 1% penicillin/streptomycin. After

reaching 100% confluence, they were cultured for another 24 h in induction medium containing 20 nM insulin, 1 nM T3, 0.5 mM isobutylmethylxanthine (IBMX, Sigma-Aldrich), 2 µg/mL dexamethasone (Sigma-Aldrich), and 0.125 mM indomethacin (Sigma-Aldrich). For differentiation, preadipocytes were grown in culture medium supplemented with 20 nM insulin (Sigma-Aldrich) and 1 nM triiodothyronine (T3) (Sigma-Aldrich). After 4 more days of culture in differentiation medium, cells exhibited a fully differentiated phenotype with massive accumulation of multilocular fat droplets. Medium was changed every day. Cells were cultured at 37°C and 8% CO₂. The cell line was tested mycoplasma free.

METHOD DETAILS

Cell transfections and treatments

Undifferentiated brown adipocytes were transfected with TARGETplus SMARTpool siRNA against *Idh3a* or *Ogdh* or control non-targeting siRNA (all at 30 nM and from Horizon Discovery) using Lipofectamine RNAiMAX transfection reagent (Thermo Fisher Scientific), according to manufacturer's instructions. Cells were analyzed 48 h after siRNA transfection.

Undifferentiated cells were transfected with plasmids (all mouse tagged ORF Clones from Origene) overexpressing *Idh2* (NM_173011), *Idh3a* (NM_029573), *Adcy10* (NM_173029), or *Ogdh* (NM_010956) or pCMV control plasmid using Lipofectamine LTX Reagent (Thermo Fisher Scientific) according to manufacturer's instructions. Cells were analyzed 48 h after plasmid transfection.

Brown adipocytes were treated with 5 µM AG-221, 1 mM acetazolamide (Sigma), 10 µM KH7 (MedChemExpress), 50 µM LRE1 (MedChemExpress), 10 µM H89 (Selleckchem), 10 µM (R)-CE3F4 (MedChemExpress), 100 µM 8-CPT-2Me-cAMP (Tocris), 10 µM CPI-613 (Cayman), 1 µM CL316,243 (MedChemExpress), 1 µM isoproterenol (Sigma) or respective controls as indicated in the figure legends. In the experiments where cells were cultured for 24 h in 0% CO₂, 25 mM HEPES was added to the medium to maintain a constant pH at 7.4.

Measurement of tricarboxylic acid cycle metabolites

TCA cycle metabolites were determined after methanol extraction by LC-MS/MS as previously described.^{37,38} Briefly, metabolites were extracted from tissues with methanol, dried, resuspended in mobile phase, and cleared with a 0.2 µm centrifugal filter. Following elution gradient was used: 99% A (0.2% formic acid in water), 1% B (0.2% formic acid in acetonitrile) for 2 min, 100% B at 2.5–2.65 min, 1% B at 3.4 min, and equilibration with 1% B until 5 min. Multiple reaction monitoring with negative electrospray ionization was used for quantification.³⁸

Isolation of mitochondria

Tissues or cells were homogenized in isolation buffer (IB) consisting of 100 mM KCl, 50 mM MOPS, 5 mM MgSO₄, 2 mM EGTA, 10 mM Na pyruvate and 10 mM K₂HPO₄ with a glass Dounce homogenizer (3× 10 strokes) on ice. Samples were centrifuged for 8 min at 600 g at 4°C, cell pellets were washed with IB, samples were centrifuged for 8 min at 600 g at 4°C, cell pellets were washed once more with IB and samples were centrifuged for 12 min at 3,200 g at 4°C. Cell pellets were resuspended in lysis buffer for cAMP measurement or for western blot. The protein content was measured using Pierce BCA Protein Assay Kit (Thermo Scientific).

cAMP measurement

cAMP amounts were measured in isolated mitochondrial fractions using a fluorometric competitive ELISA method (Abcam) following manufacturer's instructions. Fluorescence was measured using the Synergy HT microplate reader (BioTek).

Enzyme activity measurement

NAD⁺ or NADP⁺-dependent IDH and OGDH activities were measured using colorimetric assay kits (Abcam and Biomol, respectively). Absorbance was detected using the Synergy HT microplate reader (BioTek).

Seahorse analysis

OCR measurements were performed with the Seahorse XF Cell Mito Stress Test Kit using a Seahorse XF96 Analyzer (Agilent Technologies) as previously described.³⁷ Cells were plated at 80,000 cells/well in 0.2% gelatin-precoated XF96 cell culture microplate (Agilent). The experimental medium used was XF Base Medium supplemented with glucose (10 mM), pyruvate (1 mM) and glutamine (2 mM) using 2 µM Oligomycin, 2 µM FCCP (carbonylcyanide-*p*-trifluoromethoxyphenylhydrazone) and 0.5 µM Rotenone/Antimycin per manufacturer's instructions.

High-resolution respirometry

Brown adipocytes were treated for 2 h with LRE1 or (R)-CE3F4, and then they were detached from the culture plates by trypsinization. One million cells were resuspended in 100 µL Mir05 buffer (0.5 mM EGTA, 3 mM MgCl₂, 20 mM taurine (Sigma-Aldrich), 10 mM KH₂PO₄, 20 mM HEPES, 1 g/L BSA fatty acid free, 60 mM potassium-lactobionate, 110 mM sucrose, pH 7.1), and added to the chambers of the oxygraphy-O2K (Oroboros Instruments, Innsbruck, Austria) containing 1.9 mL of Mir05 buffer. Digitonin (4.05 µM, Sigma-Aldrich) was directly added to the O2K chamber simultaneously with the cells. After approximately 15 min, cells were completely permeabilized and the OCR was stabilized. Oxygen flux was monitored at the basal level and after stimulation

with 2 mM malate (Sigma-Aldrich), 5 mM pyruvate (Sigma-Aldrich), 5 mM ADP⁺Mg²⁺, and 10 mM succinate (Sigma-Aldrich). Rotenone (0.5 μM, Sigma-Aldrich), thenoyltrifluoroacetone (TTFA, 12.5 μM, Sigma-Aldrich) and finally antimycin (2.5 μM, Sigma-Aldrich) were injected to determine the oxygen consumption linked to complex I and complex II activities, respectively. For measurement of complex IV activity, 0.5 mM tetramethyl-*p*-phenylenediamine (TMPD, Sigma Aldrich) and 25 μM ascorbate (Sigma Aldrich) were added. After stabilization of the OCR, Complex IV activity was inhibited by addition of 40 mM sodium azide (Sigma Aldrich) and autooxidation of TMPD was corrected. DatLab software was used for acquisition and analysis of data.

Mitochondrial load and membrane potential assessment

Brown adipocytes were incubated with 400 nM MitoTracker Green FM or 400 nM TMRE (both from Thermo Fisher Scientific) for 30 min at 37°C in dark, as previously described.^{37,39} FACS was performed using a BD FACSCanto II (BD Biosciences) and analyzed with the BD FACSDiva Version 6.1.3 software (BD Biosciences).

Cell growth assessment

Primary brown preadipocytes were seeded at a density of 5,000 cells per well in 96 well plates. Six hours after seeding and after 1, 2, 4 and 7 days of culture, cell amounts were determined with the PrestoBlue cell viability reagent (ThermoFisher Scientific) per manufacturer's instructions. PrestoBlue cell viability reagent was added 1/10 v/v to the culture medium and cells were incubated for 1 h. Absorbance was measured at 570 nm using a microplate reader (Biotek).

Oil Red O staining

Differentiated primary brown adipocytes were washed twice with PBS, fixed with 10% formalin for 1 h, rinsed with distilled water, and stained for 1 h with Oil Red O dye (Sigma-Aldrich) in 60% isopropanol. Then, they were thoroughly rinsed with distilled water and images were acquired at bright field with an Axio Observer Z1/7 inverted microscope with Apotome mode (Zeiss) and the ZEN 3.2 blue edition software. At least 5 view-fields were imaged per sample. For quantification, the stain was extracted through incubation with 100% isopropanol for 5 min. Absorbance was measured at 492 nm using a microplate reader (Biotek).

Western blot

Tissues were lysed with 10 mM Tris-HCl, pH7.4 + 1% SDS + 1 mM sodium vanadate supplemented with protease inhibitors (cOmplete, Mini Protease Inhibitor Cocktail, Roche), cell lysates were centrifuged at 16,000 g for 5 min at 4°C, supernatants were collected and total protein concentration was measured using Pierce BCA Protein Assay Kit (Thermo Scientific). Protein samples were prepared with 5× Reducing Laemmli buffer and denatured at 95°C for 5 min or at 70°C for 10 min (the latter only for the analysis of OXPHOS proteins). Then, proteins were loaded on a 10% acrylamide gel (Invitrogen) for sodium dodecyl sulfate polyacrylamide gel electrophoresis (SDS-PAGE). PageRuler Prestained Protein Ladder (Thermo Fisher Scientific) was used as a protein size ladder. The separated proteins were transferred on Amersham Protran nitrocellulose membrane (GE Healthcare Lifescience). To verify equal protein loading, membranes were stained with Ponceau S (Sigma-Aldrich). After blocking with 5% skimmed milk in TBS-T (0.1% Tween 20 (Sigma-Aldrich) in 1x Tris-buffered saline) for 1 h at RT, membranes were incubated overnight at 4°C with anti-UCP1 (1:1,000, Abcam), anti-PGC1A (1:1,000, Merck Millipore), anti-total OXPHOS proteins (1:1,000, Abcam), anti-SDHB (1:1,000, Sigma-Aldrich), anti-β-Actin (1:1,000, Cell Signaling), or anti-Vinculin (1:1,000, Santa Cruz Biotechnology) diluted in 5% BSA in TBS-T. After washing, membranes were incubated for 1 h at RT with secondary antibodies: goat anti-rabbit IgG HRP-conjugated (1:3,000; Jackson ImmunoResearch) or goat anti-mouse IgG HRP-conjugated (1:3,000; Jackson ImmunoResearch), diluted in 5% skimmed milk in TBS-T. The signal was detected using the Western Blot Ultra-Sensitive HRP Substrate (Takara) and imaged using the Fusion FX Imaging system (PeqLab Biotechnologie).^{37,39} Band intensity was quantified with the Fiji/ImageJ software.

Quantitative RT – PCR

Total RNA was isolated from frozen BAT with the TRI Reagent (MRC) after mechanical tissue disruption, extracted with chloroform and the NucleoSpin RNA Mini kit (Macherey-Nagel). Total RNA from sorted cells was isolated with the Rneasy Plus Micro Kit (Qiagen) according to manufacturer's instructions. cDNA was synthesized with the iScript cDNA Synthesis kit (Biorad) and gene expression was determined using the SsoFast Eva Green Supermix (Bio-Rad), with a CFX384 real-time System C1000 Thermal Cycler (Bio-Rad) and the Bio-Rad CFX Manager 3.1 software, as previously described.³⁷ The relative gene expression was calculated using the $\Delta\Delta C_t$ method, 18S was used as a reference gene. Primers are listed in [Table S1](#).

QUANTIFICATION AND STATISTICAL ANALYSIS

Data are expressed as mean ± SEM. Statistical analysis was performed with Mann-Whitney U test, Student's t test or one-way ANOVA with post-hoc Tukey's test for multiple comparisons with $p < 0.05$ set as a significance level using the GraphPrism 7.04 software. Further information on data presentation and sample numbers is provided in the figure legends.